J Mater Sci (2018) 53:10822–10834

Chemical routes to materials

Highly sensitive free-base-porphyrin-based thin-film optical waveguide sensor for detection of low concentration NO_2 gas at ambient temperature

Hannikezi Abudukeremu[1], Nuerguli Kari[1], Yuan Zhang[1], Jiaming Wang[1], Patima Nizamidin[1], Shawket Abliz[1], and Abliz Yimit[1,*]

[1] College of Chemistry and Chemical Engineering, Xinjiang University, Ürümqi 830046, China

Received: 27 February 2018
Accepted: 25 April 2018
Published online: 4 May 2018

ABSTRACT

Meso-5,10,15,20-tetrakis-(4-tertbutyl phenyl) porphyrin was synthesized using Adler–Longo method and was served as sensing material. Electronic absorption spectra of the porphyrin chloroform solution and its thin film were studied comparatively. An optical waveguide sensor based on free-base porphyrin was fabricated by spin coating method. Absorption variation of porphyrin film was studied before and after exposure to NO_2, H_2S, SO_2, and volatile organic gases. XRD patterns of porphyrin film before and after exposure to analytes (NO_2, SO_2, and H_2S) were provided, and light source of the OWG testing system was selected. This facile-prepared sensor exhibited high sensitivity and selectivity to NO_2 with fast response time of 3 s and slow recovery time of 10 min or so and was capable of measuring NO_2 down to 10 ppb at ambient temperature. Scanning electron microscopy was employed to characterize film morphology before and after contact with NO_2. Film thickness was measured before (71.3 nm) and after (76.8 nm) exposure to NO_2, and film thickness variation value (5.20 nm) was calculated. The sensing behavior of the studied sensing device was tested through mixture of H_2S, SO_2, and VOC gases with NO_2 and without NO_2 for determination of the selectivity of the device. Film stability was probed by UV–Vis spectra, and response values of sensing element to NO_2 gas were detected after several days of film preparation, and its RSD value was 1.66%.

Introduction

Air pollution has become an inescapable reality in the lives of both city dwellers and villagers around the world. Therefore, air quality monitoring in both urban areas and country sides have been getting necessary in virtue of the daily massive production of harmful gases, ashes, and hydrocarbons. Such pollutants have caused negative effects on the environment, for instance, acid rain, photochemical smog, greenhouse effect, and so forth. Accordingly, there is a great demand for different types of approaches to

Address correspondence to E-mail: ablizy@sina.com

https://doi.org/10.1007/s10853-018-2374-5

detect low concentration of harmful vapors [1–4], such as NO_2, methanol, toluene, chlorobenzene. Traditional gas detection methods consist of mass spectrometry, gas chromatography, and sensors [5]. The former two suffer from disadvantages of high price, bulky volume. New gas testing approaches currently include field-effect transistors (FET_s) [4], chemical nanodevices based on dioxide graphene [6].

Nitrogen dioxide is a kind of brown red, highly active gaseous substance. The production of nitrogen dioxide mainly comes from the release of high-temperature combustion, for instance exhaust emissions from motor vehicles and power plants [7]. Nitrogen dioxide is the main damage to the respiratory system. At the initial stage of inhalation, only slight eye and upper respiratory irritation symptoms may occur in human body, such as pharynx discomfort, dry cough. [8–10]. As a result, it is very necessary to develop quantitative and qualitative detection methods. Esmaeilzadeh et al. [11] fabricated gas sensor to test NO_2 gas with different concentrations in the temperature range of 450–550 °C. Zhang et al. [12] developed field-effect transistor chemical sensors based on carbon nanotube exhibited slow response time. Plastic optical fiber (POF) sensors based on conducting graft polymer were also made to detect below 1 ppm of NO_2 in a dry atmosphere [13]. Shortcomings including elevated operating temperatures, slow response time, and sophisticated structures in these ways are obstructions to be got over. Since the 1990s, researchers have followed with interest the study and usage of optical waveguide (OWG) sensors in the domain of optical communication [14]. OWG gas sensors have been developed to measure trace amounts of detrimental gases at home and abroad [15, 16]. At present, there are few reports on the use of OWG gas sensors [17] to detect nitrogen dioxide gas even though OWG sensors possess the edges of fast response, the potentials for high sensitivity, system compactness, and intrinsically safe detection; what's more, they can be fabricated at a very low cost [18].

The type of sensitive material has great influence on the performance of sensors [19, 20], so it is important to choose the right sensitive material. As a result, there is an increasing demand for more sensitive gas-sensing compounds, which are capable of detecting toxic gases [21–24]. Organic materials are drawing tremendous attention as gas-sensing element materials owing to their low cost, easily tunable chemical structures, and ease of processing in solution to develop solid-state membranes for sensor device applications [25]. Porphyrin and related compounds have a large π-aromatic system [26], which leads to interesting optical properties [27, 28], including high optical absorption coefficient in the UV–Visible region [29]. As is known to all, when porphyrins are exposed to certain gas molecules, there occur some prominent optical and electrical changes to porphyrins [30–32]. Porphyrins have been considered as one of the most prospective sensing substances for optical gas transducers [33]. There are not many reports on the optical waveguide gas sensors based on porphyrin [17].

In this work, we report a simple realization of OWG gas sensor based on the free-base porphyrin (Fig. 1), employing spin coating process to fabricate sensing element, and investigate its sensing performance with NO_2. Film morphology was studied by SEM before and after exposure to NO_2. Film stability was observed for 20 days with UV–Vis spectroscopy, and reproducible stability of the films upon exposure to gas analyte (NO_2) was detected (2, 5, 12, 20 days after the preparation of thin films). In addition, film thickness was detected before and after exposure to certain concentration of NO_2 gas.

Experimental details

Instruments and reagents

Instruments

UV-1780 ultraviolet spectrophotometer spectroscopy (SHIMADZU, Japan); N-1100-type rotary evaporator (Beijing Oriental Science & Technology Development

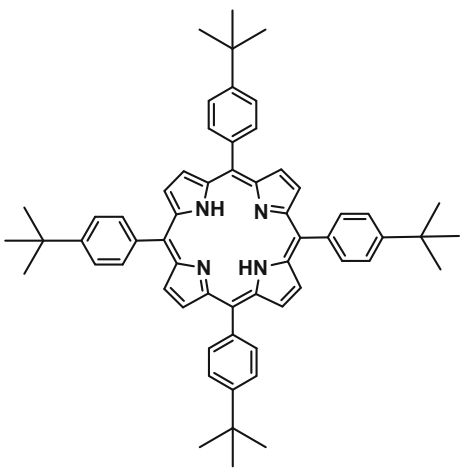

Figure 1 Chemical structure of meso-5,10,15,20-tetrakis-(4-tert-butyl phenyl) porphyrin.

Co. Ltd); SHZ-D(III) circulating water vacuum pump (Henan Gongyi yingyu Yuhua Instrument Factory); KW-4A-type spin coater (Shanghai Chemat Technology); Tin-diffused glass OWG detection system (homemade apparatus); FE-SEM (SU8019 field emission scanning electron microscope from Hitachi, Japan); thin film thickness gauge (SGC-10-type thin film thickness gauge from Tianjin Port East Technology Development Limited by Share Ltd); gas detection tube (working range: 2–200 ppm, Gastec, Beijing Municipal Institute, Beijing, China), D8-type X-ray diffraction apparatus (Bruker, Germany).

Reagents

Chloroacetic acid, pyrrole, anisole, chloroform, etc. All reagents are analytically pure and purchased from Beijing Bailingwei Technology Co. Ltd.

Preparation of porphyrin thin-film/Tin-diffused glass OWG device

Meso-5,10,15,20-tetrakis-(4-tertbutyl phenyl) porphyrin (abbreviated as porphyrin) was synthesized by Adler–longo method [34]. The electronic absorption spectra of the porphyrin chloroform solution and its thin film were studied, as given in Fig. 2. It could be observed from Fig. 2 that the UV–Vis absorption spectra of porphyrin solution in chloroform and thin film were similar, but there was a small difference in the shape of Soret band. In chloroform, porphyrin had narrow Soret band; Soret band became substantially broader when porphyrin molecules were coated on glass substrate as a thin film. Plus, the Soret band of solution and film appeared at 420, 432 nm, respectively. That is to say, the characteristic peak of porphyrin was red-shifted 12 nm after porphyrin is being paved into thin film, indicating that the head-to-tail (J-type) aggregation might be involved upon formation of porphyrin aggregates in films [35, 36]. These changes have been previously observed in porphyrin films [37–39]. In general, when the porphyrin molecules were evenly paved on glass slide, the aggregation effect was minimized and the absorption spectrum of a porphyrin film was identical with that of solution [35].

Then, certain amount of porphyrin was dissolved in 10 mL chloroform to obtain different mass percentages of porphyrin solutions. The solution was fixed on the surface of Tin-diffused glass waveguide

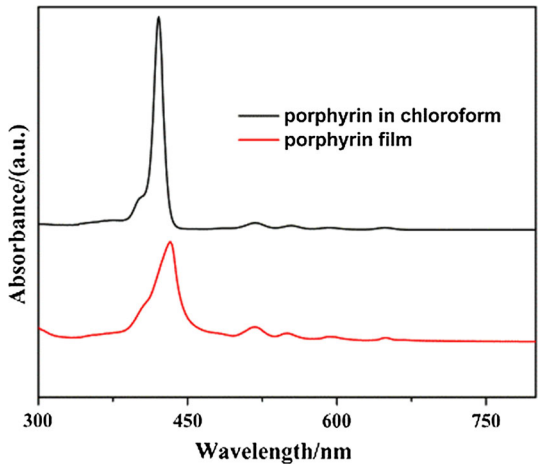

Figure 2 UV–Vis absorption spectra of porphyrin in chloroform and porphyrin thin film.

by spin coating method (about 1 cm wide porphyrin film was retained in the middle of the slide). In spin coating method, the first rotating speed of the spin coater was 450 rpm, with a rotating time of 5 s, and the second rotating speeds were 1500, 1800, and 2100 rpm, respectively, with a rotating time of 25 s. The as-fabricated OWG components were dried in vacuum circumstance for 24 h at room temperature to take sensing measurements.

Optical waveguide gas testing system

The Tin-diffused glass OWG detection system (homemade apparatus) was composed of laser, reflector, chamber, Tin-diffused glass OWG gas-sensing element, prism, photomultiplier, PC, and carrier (Fig. 3) [40]. The semiconductor laser beam (λ = 650 nm) was introduced into the waveguide layer using prism coupler [41] (glass prism, n = 1.75, matching liquid of diiodomethane as matching liquid, n = 1.74). When certain wavelength laser passed through the first prism into the Tin-diffused guided layer, light in the guided wave layer appeared in the form of the total reflection of the evanescent wave getting into the sensitive layer [42]. Intensity of the output light was monitored employing a photomultiplier detector and was kept an account of by a computer. In every measurement, a new syringe was used to inject 20 cm^3 of gas analytes onto surface of sensing element, and then out from the vent. All measurements were carried out at ambient temperature.

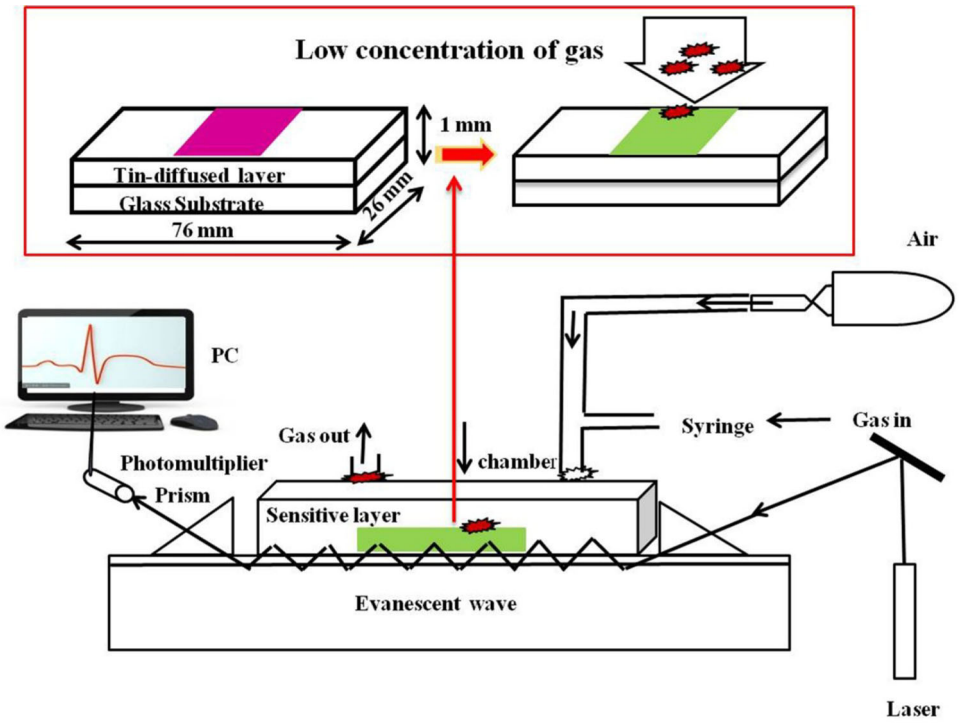

Figure 3 Schematic view of optical waveguide gas testing system.

Testing gas

Specific concentration of toluene, chlorobenzene, and other organic gases (carbon tetrachloride, methanol, ethanol, ammonia, methylamine, dimethylamine and, trimethylamine) was gained through the natural volatilization method injecting corresponding solution into a 600-mL standard vessel; according to the ideal gas equation [43]:

$$PV = nRT, \tag{1}$$

where n is the amount of substance of gas; $T = (273 + 20)K$; R is a constant of about 8.314 J/(mol K); V is volume of the standard vessel, which is equal to V_{gas}; and P represents saturated vapor pressure of volatile organic compounds (at 20 °C), it is inferred that the amount of volatile organic compound measured in standard vessel remains unchanged after its natural volatilization. In other words, n is certain. And since $n = \frac{m}{M}$, $m = \rho V_{liquid}$, ρ is density of the liquid at 20 °C; M is molecular weight of the volatile organic compound; m stands for quality of volatile organic compound. So:

$$PV_{gas} = nRT = \frac{RT\rho V_{liquid}}{M} \tag{2}$$

$$V_{liquid} = \frac{PV_{gas}M}{RT\rho} \tag{3}$$

$$C_{gas} = \frac{n}{V_{gas}} = \frac{m}{MV_{gas}} \tag{4}$$

And there exists a relation between C_{gas} and ppm value [44]:

$$ppm = \frac{22.4 * C_{gas}}{M} \tag{5}$$

Certain amount of copper powder was weighed into the same specification vessel; then, certain amount of concentrated nitric acid was added to prepare specific concentration of NO_2 gas; SO_2 was obtained through the reaction between a certain amount of sodium sulfite and concentrated hydrochloric acid; H_2S was obtained via the reaction between a certain amount of ferrous sulfide and concentrated hydrochloric acid. Different amounts of standard target gases were deliquated with pure air to get desired concentrations in the second 600 mL standard vessel: A certain amount of standard target gas from the first standard vessel is injected into the second standard vessel to obtain lower concentration of gas analytes by syringe and then diluted with pure air. The amount of gas (n) in this dilution process is certain. By this way, very low concentrations of analyte gases were achieved. In order to verify the

accuracy of the gas concentration, gas concentration in the standard vessel is detected by gas tube after complete volatilization of the liquid (VOCs) and after complete reaction of reagents (inorganic gases).

Results and discussion

Detecting principle

In an optical waveguide sensor, interactivity between the sensitive film and measured gases would cause slight changes in optical property (transmittance or absorbance) of the sensitive film, which will give rise to great changes of output light intensity that is related to absorbance and thickness of the film [45]:

$$I = I_0(1 - \alpha N d_e) \quad (6)$$

In this calculation, I is output light intensity, I_0 stands for input light intensity, α denotes absorbance coefficient of the sensitive film, N is refractive numbers of the guided light on the surface of OWG with length L, and d_e represents the real distance of light propagation, respectively. This relation indicates that when absorbance coefficient of the sensitive layer increases (α), output light intensity will decrease; the intensity of output light will increase when the absorption coefficient of sensitive layer decreases. In this experiment, dry air played roles of carrier and dilution gas. Before testing starts, dry air is introduced into the system and baseline is still stable. When the measured gas enters the chamber, interaction between the measured gas and sensitive elements may occur, which may be chemical reaction or physical absorption or neither. When the interaction occurs between the measured gas and sensitive element, it either absorbs a part of the incident light or reflects the incident light or neither absorbs nor reflects the input light. When the light is absorbed (α increases), the output light intensity decreases, while the reflected light leads to the enhancement of output light intensity (α decreases); when sensing element does not interact with the measured object, the output light intensity remains unchanged (α unchanged), that is, the baseline is stable [46, 47].

UV-visible spectroscopy

Porphyrin film coated on glass slide was exposed to toluene, chlorobenzene and other volatile organic compounds (VOCs) and NO_2, H_2S, and SO_2 gases, and absorbance of the film was tested before and after exposure to gas analytes (as depicted in Fig. 4). These results are given in Table 1. Detection of absorbance was performed by an ultraviolet spectrophotometer spectroscopy. When porphyrin films were exposed to VOCs, there were no palpable changes in absorbance of the film; while porphyrin films were exposed to those three kinds of inorganic gases, the Soret band was red-shifted and four characteristic Q peaks generated to one stronger peak; absorbance of the film was augmented in the range of 610–750 nm. At 650 nm, the changes of film absorbance induced by NO_2, H_2S, and SO_2 gases were 0.0257, 0.0167, 0.0165 nm, respectively. At the same wavelength, maximum absorbance change value was caused by NO_2. Besides, when porphyrin membranes were contacted with those three kinds of inorganic gases, the color of the membrane changed from purple to green (as shown in Fig. 3).

The XRD patterns of the film before and after exposure to analytes (NO_2, SO_2, and H_2S) at 2θ values from 5 to 80 are given in Fig. 5. The diffraction peak position of the thin film was basically unchanged after contacting with the measured gases, while the diffraction peak intensity of the film varied after contacting with the measured gases. When exposed to NO_2, intensity of the strong diffraction peak of the

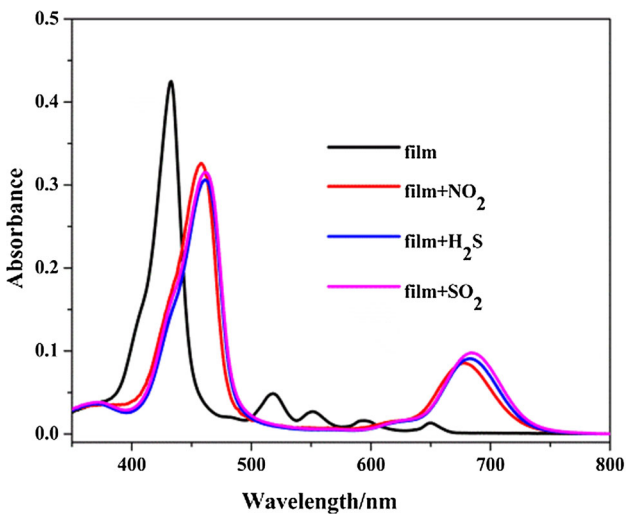

Figure 4 UV–Vis absorption spectra of film and its change after exposure to certain concentration of several inorganic gases.

Table 1 Absorbance change of sensitive film after exposure to certain concentration of several inorganic gases

Abs.	Abs. (650 nm)	$\Delta Abs. = Abs._{(exposure)} - Abs_{(film)}$
Film	0.0132	0.0000
Film + NO_2	0.0389	0.0257
Film + H_2S	0.0299	0.0167
Film + SO_2	0.0297	0.0165

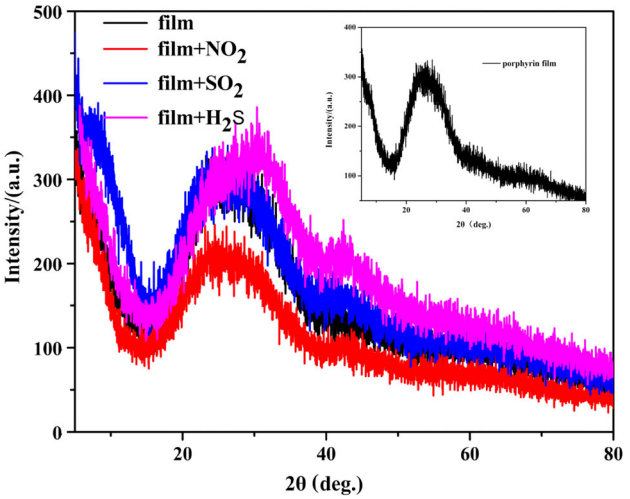

Figure 5 XRD patterns of porphyrin film before and after exposure to analytes.

film suffered from decrease (peak intensity variation value was about 90); exposed to SO_2, there was no palpable changes in film XRD patterns; exposed to H_2S, there emerged an increase in intensity of the strong diffraction peak of the film and shift to higher 2θ values compared with film. Based on the above changes, we can speculate that the crystallinity of the films changed after contacting with the measured gases. Plus, it was worth mentioning that after the contact with those three kinds of analytes, the bending degree of film's XRD diffraction peak was more obvious at $40°\theta$. Combining the UV absorption spectrums and XRD patterns of the thin film before and after exposure to those three kinds of analytes, it could be deduced that change of thin film caused by NO_2 was larger than that of the other two.

Gas exposure

Porphyrin thin-film/Tin-diffused glass OWG elements were immobilized in OWG gas testing system for exposure to VOCs and the three kinds of inorganic gases. Responses of the porphyrin-based glass OWG sensor to 100 ppm VOCs and three kinds of inorganic gases were measured, which are directly related to thickness of the sensitive film, and film thickness has something to do with concentration of solutions and rotating speeds of spin coater [48, 49]. Thus, solution concentrations and rotating speeds were optimized (Fig. 6). Signal change was calculated through the following formula [42]:

$$\Delta I(\text{signal intensity change}) = I_{\text{gas}} - I_{\text{air}}, \quad (7)$$

where I_{gas} denotes output light intensity in the gas, while I_{air} is output light intensity in the surrounding air. As displayed in Fig. 6, when exposed to VOCs, sensing element had exhibited relatively small responses to all VOCs compared with inorganic gases. Plus, among those three kinds of inorganic gases, sensing component had showed much larger response to NO_2 than the other two kinds of vapors. The porphyrin sensing elements under different conditions (diverse mass concentrations with diverse rotating speeds) displayed responses to the selected analytes, among which sensing element with mass concentration of 0.07% and rotating speed of 1800 rpm exhibited the best response to the NO_2 vapor (Fig. 6b). Signal intensity change value (ΔI) for NO_2 gas ran up to 650 (maximum variation value) at room temperature upon that condition (under mass concentration of 0.07% and rotating speed of 1800 rpm). Hence, it could be determined that this condition was the best condition for preparation of sensitive films to achieve better sensitive layer. Then, further measurements all were carried out under the best condition. From Fig. 6, it was not difficult to find out that sensing component showed a little response to VOCs. So in our later work, we had selected five VOCs as analytes to conduct further detection (Fig. 7). In addition, upon exposed to NO_2 or H_2S or SO_2 gas, as-described device showed fast responses to these three inorganic gases with slow recovery times; no matter which gas was in contact with the element, color of the film changed from purple to green, making it difficult to carry out continuous online test for these three gases upon the same one element. The as-described device showed higher response to NO_2 compared with H_2S and SO_2. Furthermore, based on the UV–Vis absorption spectra and XRD patterns of porphyrin film before and after exposure to those three kinds of gases (changes caused by NO_2 were more obvious than the other

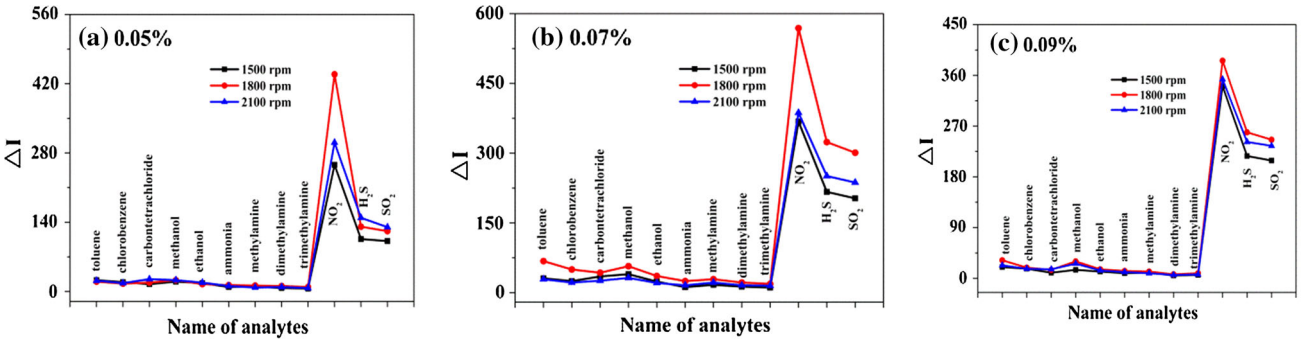

Figure 6 Line chart of preparation conditions of the porphyrin-based Tin-diffused film optical waveguide device prepared with various rotating speeds 1500–2100 rpm: **a**–**c** where films were developed from porphyrin solution with mass concentration of 0.05, 0.07, 0.09%, respectively.

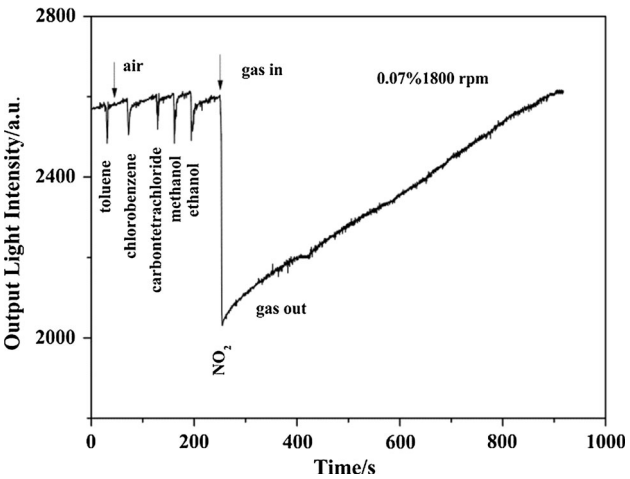

Figure 7 Dynamic response curve of the porphyrin thin-film Tin-diffused glass OWG sensor to 100 ppm gas analytes.

two), we selected NO_2 as analyte together with the five VOCs mentioned above to take dynamic measurement in our homemade testing system.

In this work, selectivity response of the as-presented OWG element to selected gases was measured by applying a semiconductor laser beam illuminant. As displayed in Fig. 7, in the process of gas measurement, as described above, dry air was functioned as carrier and dilution gas; it was made to transfer the measured gas to the chamber. When air was introduced into the system, baseline was still stable. The response time is perceived as the time required to reach 90% of the equilibrium value following exposure to the measured gas, and recovery time is seen as the time required for sensing element to return to within 10% of the initial response in air when release of the gas [50]. Described sensitive device exhibited fast, strong response to selected objects, especially to the NO_2. Upon exposed to the former five kinds of 100 ppm VOCs, device showed fast response and recovery times within a few seconds. While exposed to the same concentration of NO_2, device also revealed fast response time (3 s), but slow recovery time (10 min or so, Fig. 7). It can be estimated from Fig. 7, in which signal change of NO_2 (ΔI = 650) was five times more than that of other gases. We also could infer that the sensing device revealed good selectivity and high sensitivity to NO_2. Intensity of the output light reduced with the existence of the object analyte (NO_2) as displayed in Fig. 7. As given in Fig. 4, porphyrin sensitive film was exposed to measured gas (NO_2), which resulted in an increase of absorbance (at 650 nm) of the sensitive film. It indicated that interaction between sensitive material and measured gas triggered augment of light absorption (α increased). Therefore, when the light passes through surface of the sensitive element, interaction between sensitive element and NO_2 caused absorption of some incident light, which brought decrease of the output light intensity. This result showed in accordance with Eq. (6). Another point worth mentioning is that the optical waveguide gas sensor has the characteristic of fast response. Hence, there may be sudden change in light intensity.

It is necessary to go a step further in verification of porphyrin sensing element's selectivity to NO_2. Hence, two kinds of gas mixtures were prepared: In the first group, there were toluene, chlorobenzene, carbon tetrachloride, methanol, ethanol, H_2S, SO_2, and NO_2; in the second group, there contained all the gases in the first group except for NO_2; and concentration of each gas was 100 ppm. As shown in Fig. 8a, b, when in contact with mixed gas containing NO_2,

as-prepared testing device revealed much bigger output light intensity than that of contact with pure NO_2, indicating that the sensitive element also had a certain response to other gases, which caused increase in signal intensity. What's more, the response of sensitive element to gas mixture containing NO_2 was larger than that of gas mixture that did not contain NO_2. It could be deduced that as-mentioned sensitive element did have a selective response to NO_2.

In the interest of study correlation between NO_2 concentration and response of porphyrin OWG element to NO_2, elements were exposed to 100, 10, 1 ppm, 100, and 10 ppb NO_2 under the selected best condition, respectively. With the increase of NO_2 concentration, output light intensity was reduced, implying concentration dependency performance of sensing device (Fig. 9).

The response strength was calculated by Eq. (7). Corresponding response of sensing element was achieved even upon exposure to low concentration of NO_2 (10 ppb) (Fig. 9). It is noticeable that there was a good linear relationship between gas concentration and light intensity variation value.

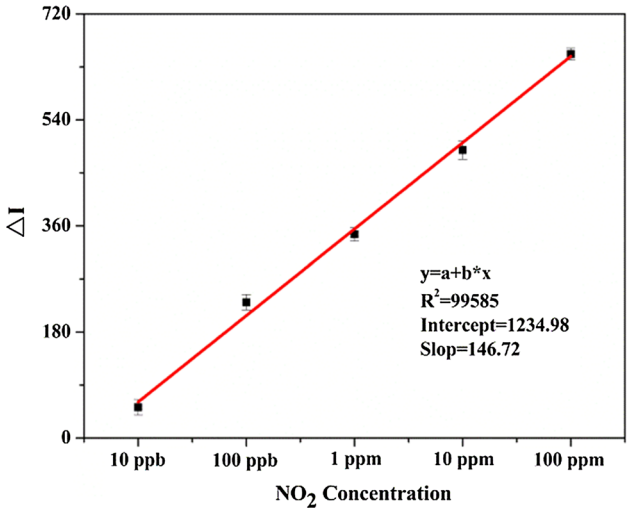

Figure 9 Linear relationship diagram of light intensity variation value of OWG sensing element upon exposure to different concentration of NO_2.

Characterization of the sensitive film

It is well known that efficiency of gas sensor is greatly dependent on the structure of sensing materials [51]. Due to its large specific surface area, high porosity, and excellent accessibility for gaseous analytes, porous structure is highly attractive to sensing materials [52]. Prepared porphyrin film was characterized by FE-SEM, and results are given in Fig. 10. It can be seen from Fig. 10a that surface of the film has presented irregular multi-pore structures, and pore sizes were between 37 and 68 nm, which were in the mesoporous and large pore range. And these disordered hole structures are beneficial to gas adsorption [53, 54], which increases the reaction between gas molecules and sensing films [55]. As displayed in Fig. 10b, upon exposure to NO_2 gas, film morphology was different from the former, and multi-hole structures were not very obvious compared with Fig. 10a, emerging many cracks on surface of the film, which was maybe that NO_2 gas was absorbed by described disorganized porous structures, altering surface of the film. Then, that might be the reason why the sensing element presented long recovery time.

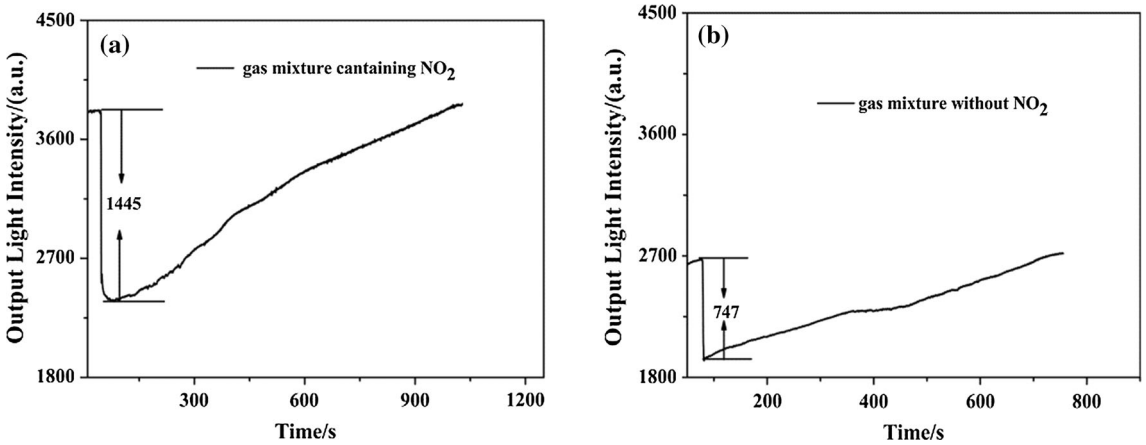

Figure 8 Dynamic response curve of the porphyrin thin-film Tin-diffused glass OWG sensor to gas mixture with NO_2 and without NO_2.

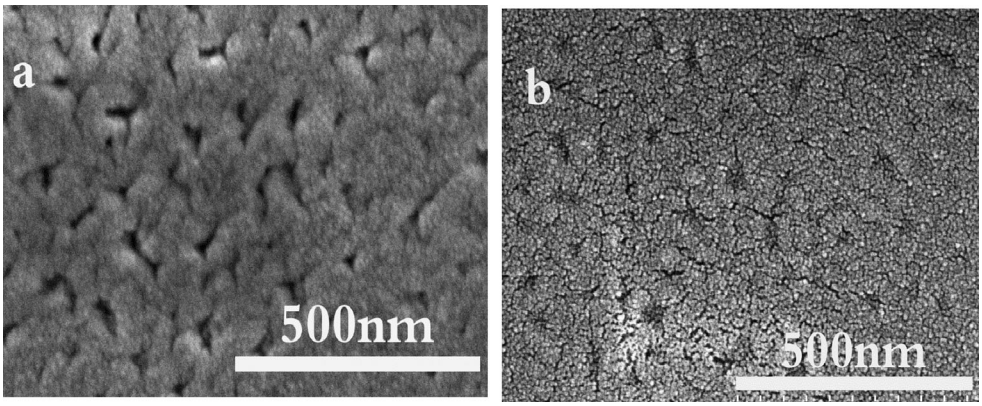

Figure 10 SEM images of film before (**a**) and after (**b**) exposure to NO_2 gas.

In order to better describe properties of sensitive membrane (under the best sensing condition mentioned above), thickness of thin film was measured by thin film thickness gauge. Five points were selected on surface of the film before and after exposure to NO_2 gas, and average thicknesses of the film before and after exposure were 71.3 and 76.8 nm, respectively (Table 2). After exposure to NO_2 gas, there was an increment in film thickness and average thickness variation of membrane was 5.5 nm, which could imply that NO_2 gas was taken up by the membrane. This result was well matched with SEM images of the film.

Contact of porphyrin film with NO_2, SO_2, H_2S resulted in disappearance of characteristic Soret band of porphyrin and emerging of a novel band about 458 nm (Fig. 4), which was in accordance with reports from other researchers applying distinct free-base porphyrins [45, 56–58]. These spectral changes were well put down in many documents, and in view of the fact that porphyrins are electron-rich substances and NO_2 is a strong oxidizing material, a charge transfer process in the form of oxidation is the most probable mechanism for such behavior [59–61], which can be described in Fig. 11. SO_2 is also a oxidizing agent, of which oxidizing capacity is lower than that of NO_2 [62, 63], so there may be the same mechanism between porphyrin and SO_2 [64]. The reaction mechanism can be divided into two procedures. In the first procedure, porphyrin was oxidized by NO_2. This brings about changes in the infrared, but not in the visible range; in the second procedure, another NO_2 molecule reacts covalently with the reaction product of the first procedure and the second step stimulates the color variation from purple to green. This makes them pleasant campaigners for one-time use of NO_2 transducer. And for H_2S, there was the same phenomenon when in contact with porphyrin film. Unlike the former two, H_2S is a reducing substance [65], and according to some studies, metalloporphyrins can oxidize H_2S [66, 67]. However, there are no relevant papers to explain the reaction mechanism between free-base porphyrin and H_2S, employing redox reaction. According to interaction mechanism between metalloporphyrins and H_2S, we suppose that porphyrin may act as oxidant when in contact with H_2S. Further efforts are still needed to explain the mechanisms of the interactions between porphyrin and these gases.

Film stability was probed by recording membrane UV–Vis spectra till 20 days from preparation of the membrane (Fig. 12, left). During this period, specimen was kept in the dark to prevent from contacting with pollutant gases. Influence of time on porphyrin

Table 2 Film thickness and its variation after exposure to NO_2

	1	2	3	4	5	Average thickness (nm)
Film thickness (nm)	71.3	71.5	72.9	71.3	71.3	71.3
Film thickness after exposure to NO_2 (nm)	77.6	76.2	78.6	76.7	75.2	76.8
Film thickness variation (nm)	6.30	4.70	5.70	5.40	3.90	5.20

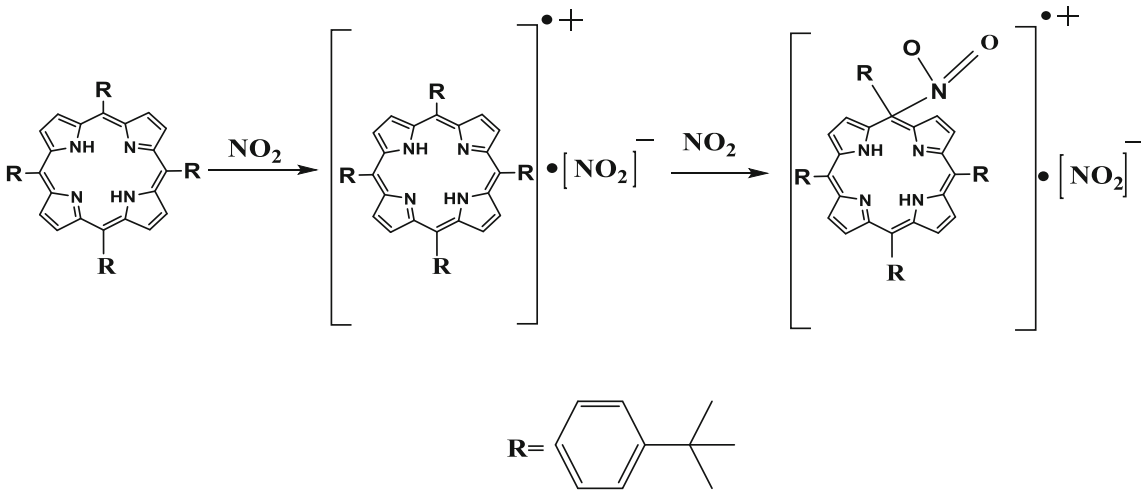

Figure 11 Reaction mechanism diagram of porphyrin to NO_2.

film had produced one notable result. Film presented an increase in absorbance intensity, which may be attributed to volatilization of solvent in porphyrin film. Shape of the spectra upon 20 days had showed no changes. As drawn in Fig. 12 (right), the response values of sensing element to NO_2 gas were detected after several days of film preparation (2, 5, 12, 20 days after the preparation of thin films), and the RSD value was 1.66%. According to Fig. 12, it could be inferred that the film was fairly stable and had good reproducibility.

Conclusion

A free-base porphyrin-based planar OWG sensor has been developed by spin coating method. UV–Vis spectra of the porphyrin solution and its film had been compared. The sensor element exhibited good sensitivity to selected analytes and selectivity to NO_2 gas with fast response time and slow recovery time. When in contact with NO_2, H_2S, and SO_2, the color of the porphyrin film changed from purple to light green. SEM image results of the film before and after exposure to NO_2 had exhibited an accordance with the film thickness variation. And as-mentioned sensing element could detect very low concentration of NO_2 with detection limit of 10 ppb. In order to highlight the selectivity of the sensing element to NO_2, the mixed gases with NO_2 and without NO_2

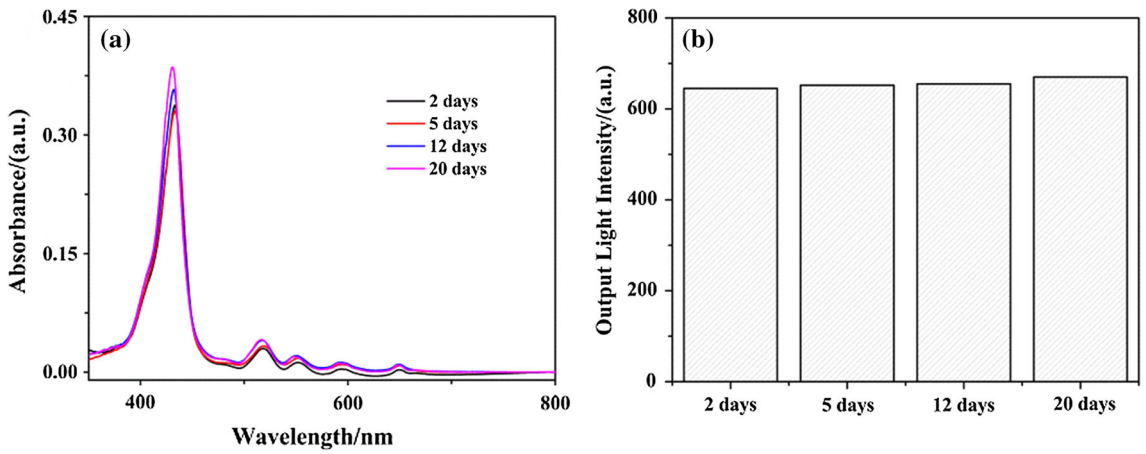

Figure 12 UV–Vis absorption spectra of porphyrin film (2, 5, 12, 20 days after the preparation of thin films) and response values of sensing element to NO_2 (2, 5, 12, 20 days after the preparation of thin films).

were tested; the results showed that the response of the sensing element to the mixed gases with NO_2 was much larger than that of without NO_2. The reaction mechanism was explained in detail by oxidation–reduction reaction. Compared with other sensors, the prepared porphyrin thin-film/Tin-diffused glass optical waveguide element has merits of low cost, simple structure, easy preparation, high sensitivity, and fast response and will pave a path for the exploration of optical sensors.

Acknowledgements

This work was supported by the National Science Foundation of China (Grant No. 21765021).

References

[1] Teoh LG, Hon YM, Shieh J, Lai WH, Hon MH (2003) Sensitivity properties of a novel NO_2 gas sensor based on mesoporous WO_3 thin film. Sens Actuators B Chem 96(1–2):219–225

[2] Chung MG, Kim DH, Lee HM, Kim T, Choi JH, Seo DK, Yoo JB, Hong SH, Kang TJ, Kim YH (2012) Highly sensitive NO_2 gas sensor based on ozone treated graphene. Sens Actuators B Chem 166–167(6):172–176

[3] Swanson JJ, Watts WF, Newman RA, Ziebarth RR, Kittelson DB (2013) Simultaneous reduction of particulate matter and $NO_{(x)}$ emissions using 4-way catalyzed filtration systems. Environ Sci Technol 47(9):4521–4527

[4] Andringa AM, Piliego C, Katsouras I, Blom PWM, Leeuw DMD (2014) NO_2 detection and real-time sensing with field-effect transistors. Chem Mater 26(1):773–785

[5] Dakin JP, Chambers P (2006) Review of methods of optical gas detection by direct optical spectroscopy, with emphasis on correlation spectroscopy. Springer, New York, pp 457–477

[6] Santos JP, Polichetti T, Aleixandre M, Hontañón E, Sayago I, Alfano B, Miglietta ML, Francia GD (2017) Tin dioxide-graphene based chemi-device for NO_2 detection in the sub ppm range. Proceedings. https://doi.org/10.3390/proceedings1040442

[7] Wang Y, Ma P, Song F, Yao S, Chen C, Zhu P (2017) Comparative NO_2-sensing in cobalt and metal-free porphyrin nanotubes. J Colloid Interface Sci 490:129–136

[8] Ou JZ, Ge WY, Carey B, Daeneke T, Rotbart A, Shan W, Wang YC, Fu ZQ, Chrimes AF, Wiodarski W, Russo SP, Li YX, Kalantar-zadeh K (2015) Physisorption-based charge transfer in two-dimensional SnS_2 for selective and reversible NO_2 gas sensing. ACS Nano 9(10):10313–10323

[9] Guarnieri M, Balmes JR (1996) Outdoor air pollution and asthma. Food Chem Toxicol Int J Publ Br Ind Biol Res Assoc 34(3):318–319

[10] Manta DS (2000) Air pollution and health in urban areas. Rev Environ Health 15(1–2):13–42

[11] Esmaeilzadeh J, Marzbanrad E, Zamani C, Raissi B (2012) Fabrication of undoped-TiO_2 nanostructure-based NO_2 high temperature gas sensor using low frequency AC electrophoretic deposition method. Sens Actuators B Chem 161(1):401–405

[12] Zhang J, Boyd A, Tselev A, Paranjape M, Barbara P (2006) Mechanism of NO_2 detection in carbon nanotube field effect transistor chemical sensors. Appl Phys Lett 88(12):123112–123113

[13] Maciak E, Sufa P, Stolarczyk A (2014) A low temperature operated NO_2 gas POF sensor based on conducting graft polymer. Photonics Lett Pol 6(4):124–126

[14] Ito K, Fujishima A (1988) An application of optical waveguides to electrochemistry: construction of optical waveguide electrodes. J Phys Chem 92(25):7043–7045

[15] Nizamidin P, Yimit A, Abdurrahman A, Itoh K (2013) Formaldehyde gas sensor based on silver-and-yttrium-co doped-lithium iron phosphate thin film optical waveguide. Sens Actuators B Chem 176(6):460–466

[16] White IH, Bamiedakis N, Penty R, Elliott SR, Hutter T (2013) PCB-integrated optical waveguide sensors: an ammonia gas sensor. J Lightwave Technol 31(10):1628–1635

[17] Peter C, Schmitt K, Apitz M, Woellenstein J (2012) Metallo-porphyrin zinc as gas sensitive material for colorimetric gas sensors on planar optical waveguides. Microsyst Technol 18(7–8):925–930

[18] Yimit A, Itoh K, Murabayashi M (2003) Detection of ammonia in the ppt range based on a composite optical waveguide pH sensor. Sens Actuators B Chem 88(3):239–245

[19] Yin L, Chen D, Zhang H, Shao G, Fan B, Zhang R, Shao G (2014) In situ formation of Au/SnO_2 nanocrystals on WO_3 nanoplates as excellent gas-sensing materials for H_2S detection. Mater Chem Phys 148(3):1099–1107

[20] Yuan CL, Chang CP, Hong YS, Sung Y (2009) Fabrication of MWNTs-PANI composite—a chemiresistive sensor material for the detection of explosive gases. Mater Sci Pol 27(2):509–520

[21] Choudhuri I, Sadhukhan D, Garg P, Mahata A, Pathak B (2016) Lewis acid-base adducts for improving the selectivity and sensitivity of graphene based gas sensors. ACS Sens 1(4):451–459

[22] Hou C, Li J, Huo D, Luo X, Dong J, Yang M, Shi X (2012) A portable embedded toxic gas detection device based on a cross-responsive sensor array. Sens Actuators B Chem 161(1):244–250

[23] Lei J, Hou C, Huo D, Li Y, Luo X, Yang M, Fa H, Bao M, Li J, Deng B (2016) Detection of ammonia based on a novel fluorescent artificial nose and pattern recognition. Atmos Pollut Res 7(3):431–437

[24] Gyger F, Hübner M, Feldmann C, Barsan N, Weimar U (2010) Nanoscale SnO_2 hollow spheres and their application as a gas-sensing material. Chem Mater 22(16):4821–4827

[25] Evyapan M, Dunbar ADF (2015) Improving the selectivity of a free base tetraphenylporphyrin based gas sensor for NO_2 and carboxylic acid vapors. Sens Actuators B Chem 206(206):74–83

[26] Paolesse R, Nardis S, Monti D, Stefanelli M, Di NC (2017) Porphyrinoids for chemical sensor applications. Chem Rev 117(4):2517–2583

[27] Richardson TH, Dooling CM, Jones LT, Brook RA (2005) Development and optimization of porphyrin gas sensing LB films. Adv Colloid Interface Sci 116(1–3):81–96

[28] Richardson TH, Dooling CM, Worsfold O, Jones LT, Kato K, Shinbo K, Kaneko F, Tregonning R, Vysotsky MO, Hunter CA (2002) Gas sensing properties of porphyrin assemblies prepared using ultra-fast LB deposition. Colloids Surf A Physicochem Eng Asp 198–200(4):843–857

[29] Fagadar-Cosma E (2007) UV–Vis and fluorescence spectra of meso-tetraphenylporphyrin and meso-tetrakis-(4-methoxyphenyl) porphyrin in thf and thf-water systems. The influence of pH. Rev Chim Buchar 58(5):451–455

[30] Gutiérrez AF, Brittle S, Richardson TH, Dunbar A (2014) A proto-type sensor for volatile organic compounds based on magnesium porphyrin molecular films. Sens Actuators B Chem 202(10):854–860

[31] Kerdcharoen T, Kladsomboon S (2013) Optical chemical sensor and electronic nose based on porphyrin and phthalocyanine. Springer 14:237–255

[32] Beswick RB, Pitt CW (1988) Optical detection of toxic gases using fluorescent porphyrin langumuir—blodgett films. J Colloid Interface Sci 124(1):146–155

[33] Okura I (2009) Overview of optical sensors using porphyrins. J Porphyr Phthalocyanines 6(04):268–270

[34] Yong QI, Huang YJ, Pan JG (2014) Synthesis of meso-5,10,15,20-tetrakis(4-isopropylphenyl) porphyrin and its metalloporphyrins. Chin J Chem Reag 36(6):493–496

[35] Luo L, Lo CF, Lin CY, Chang IJ, Diau EW (2006) Femtosecond fluorescence dynamics of porphyrin in solution and solid films: the effects of aggregation and interfacial electron transfer between porphyrin and TiO_2. J Phys Chem B 110(1):410–419

[36] Tokunaga E, Nakata K (2012) Giant electrooptic effect of porphyrin. J-Aggregates 2:213–246. https://doi.org/10.1142/9789814365796-0008

[37] And JLH, Kuciauskas Darius (2008) Contrasting Fe(III) tetrakis(4-hydroxyphenyl) porphyrin excited state dynamics in solution and solid states. J Phys Chem C 112(5):1700–1704

[38] Dolci LS, Marzocchi E, Montalti M, Prodi L, Monti D, Di NC, D'Amico A, Paolesse R (2006) Amphiphilic porphyrin film on glass as a simple and selective solid-state chemosensor for aqueous Hg^{2+}. Biosens Bioelectron 22(3):399–404

[39] Sales NFD, Mansur HS (2008) Chemsensor of NO_2 gas based on porphyrin of 5, 10, 15, 20-tetraphenylporphyrin LB films and LS films. Mater Res 11(4):477–482

[40] Nizamidin P, Yimit A, Nurulla I, Itoh K (2014) Optical waveguide BTX gas sensor based on yttrium-doped lithium iron phosphate thin film. Isrn Spectrosc. https://doi.org/10.5402/2012/606317

[41] Kadir R, Yimit A, Ablat H, Mahmut M, Itoh K (2009) Optical waveguide BTX gas sensor based on polyacrylate resin thin film. Environ Sci Technol 43(13):5113–5116

[42] Zhu M, Kari N, Yan Y, Yimit A (2017) Fabrication and gas sensing application of fast-responding m-CP-PVP composite film/potassium ion-exchanged glass optical waveguide. Anall Methods 9(37):5494–5501

[43] Houri A, Wehbe H (2003) Towards an environmentally friendly chemistry laboratory: managing expired chemicals. Green Chem 5:285–290. https://doi.org/10.1039/b305234f

[44] Liang Lingfeng, Zhong Jianhui (2017) The application of simplified formula for conversion of pollutants concentration between unit ppm and mg/m^3 in fixed pollution sources. Chin J Resour Econ Environ Prot 5:104

[45] Tuerdi G, Kari N, Yan Y, Nizamidin P, Yimit A (2017) A functionalized tetrakis(4-nitrophenyl)porphyrin film optical waveguide sensor for detection of H_2S and ethanediamine gases. Sensors 17(12):2717. https://doi.org/10.3390/s17122717

[46] Mahmut M, Yimit A, Abudukayum A, Mamut M, Itoh K (2008) Highly sensitive and selective optical HCl gas sensor based on polymer thin film with immobilized Congo red. Sens Lett 6(2):290–293

[47] Abdurahman R, Yimit A, Ablat H, Mahmut M, Wang JD, Itoh K (2010) Optical waveguide sensor of volatile organic compounds based on PTA thin film. Anal Chim Acta 658(1):63–67

[48] Le QB, Chang HS, Ahn KS, Kim JH, Thogiti S (2017) Effect of LiI/I_2 concentration and photoelectrode thickness on the photovoltaic properties of NiO-based p-type dye-sensitized solar cells. Mol Cryst Liq Cryst 653(1):99–108

[49] Zulkapli NN, Abd Manaf ME, Ab Maulod HE, Abdul Manaf NS, Raja Seman RNA, Bistamam MSA, Talib E, Azam MA (2015) Control of cobalt catalyst thin film thickness by varying spin speed in spin coating towards carbon nanotube growth. Appl Mech Mater 761:421–425

[50] Alsaif MM, Field MR, Murdoch BJ, Daeneke T, Latham K, Chrimes AF, Zoolfakar AS, Russo SP, Ou JZ, Kalantarzadeh K (2014) Substoichiometric two-dimensional molybdenum oxide flakes: a plasmonic gas sensing platform. Nanoscale 6(21):12780–12791

[51] Sun X, Bruckner C, Nieh MP, Lei Y (2014) A fluorescent polymer film with self-assembled three-dimensionally ordered nanopores: preparation, characterization and its application for explosives detection. J Mater Chem A 2(35):14613–14621

[52] Hu M, Kang W, Zhao Y, Shi J, Cheng B (2017) A fluorescent and colorimetric sensor based on a porphyrin doped polystyrene nanoporous fiber membrane for HCl gas detection. RSC Adv 7(43):26849–26856

[53] Lin FW, Xu XL, Wan LS, Wu J, Xu ZK (2015) Porphyrinated polyimide honeycomb films with high thermal stability for HCl gas sensing. RSC Adv 5(39):30472–30477

[54] Shi JT, Yue KF, Liu B, Zhou C, Liu YL, Fang ZG, Wang YY (2014) Two porous metal–organic frameworks (MOFs) based on mixed ligands: synthesis, structure and selective gas adsorption. CrystEngComm 16(15):3097–3102

[55] Navale ST, Mane AT, Chougule MA, Sakhare RD, Nalage SR, Patil VB (2014) Highly selective and sensitive room temperature NO_2 gas sensor based on polypyrrole thin films. Synth Met 189(189):94–99

[56] Jagadeeswari S, Paramaguru G, Renganathan R (2014) Synthesis and characterization of free base and metal porphyrins and their interaction with CdTe QDs. J Photochem Photobiol A Chem 276:104–112

[57] Scamporrino E, Mineo P, Vitalini D (2011) Covalent nano-clip and nano-box compounds based on free base porphyrins. Tetrahedron 67(20):3705–3713

[58] Wohrle D (1997) The colours of life. An introduction to the chemistry of porphyrins and related compounds. Adv Mater 9(15):1191–1192

[59] Roales J, Pedrosa JM, Guillén MG, Lopes-Costa T, Castillero P, Barranco A, González-Elipe AR (2015) Free-base carboxyphenyl porphyrin films using a TiO_2 columnar matrix: characterization and application as NO_2 sensors. Sensors 15(5):11118–11132

[60] Gulino Antonino, Mineo Placido, Scamporrino Emilio, Daniele Vitalini A, Fragalà Ignazio (2004) Molecularly engineered silica surfaces with an assembled porphyrin monolayer as optical NO_2 molecular recognizers. Chem Mater 16(16):1838–1840

[61] Cao D, Deng J, Li H, Wang L (2013) Recent advances in porphyrin-derived sensors. Curr Organ Chem 17(24):3078–3091

[62] Lee YN, Schwartz SE (1982) Kinetics of oxidation of aqueous sulfur (IV) by nitrogen dioxide. Precip Scav Dry Depos Resuspens 1:453–470

[63] Stevens DK (2010) Method for reducing the H_2S content of an H_2S-containing subterranean formation. http://www.freshpatents.com/-dt20100506ptan20100108315.php. Accessed 08 Apr 2018

[64] Wu K, Guo J, Wang C (2014) Dispersible and discrete metalloporphyrin-based CMP nanoparticles enabling colorimetric detection and quantitation of gaseous SO_2. Chem Commun 50(6):695–697

[65] Boll W, Nehb W, Jüngst E (2010) Apparatus and method for operating the apparatus for continuously recovering sulfur from gas containing H_2S. http://xueshu.baidu.com/s?wd=paperuri%3A%2811e1508efdce7ba321969aed75917b5a%29&filter=sc_long_sign&tn=SE_xueshusource_2kduw22v&sc_vurl=http%3A%2F%2Fwww.freepatentsonline.com%2F7776308.html&ie=utf-8&sc_us=11985111192211831645. Accessed 08 April 2018

[66] Mirra S, Milione S, Strianese M, Pellecchia C (2015) A copper porphyrin for sensing H_2S in aqueous solution via a "coordinative-based" approach: a copper porphyrin for sensing H_2S in aqueous solution. Eur J Inorg Chem 13:2272–2276

[67] Pavlik JW, Noll BC, Oliver AG, Schulz CE, Scheidt WR (2010) Hydrosulfide (HS^-) coordination in iron porphyrinates. Inorg Chem 49(3):1017–1026